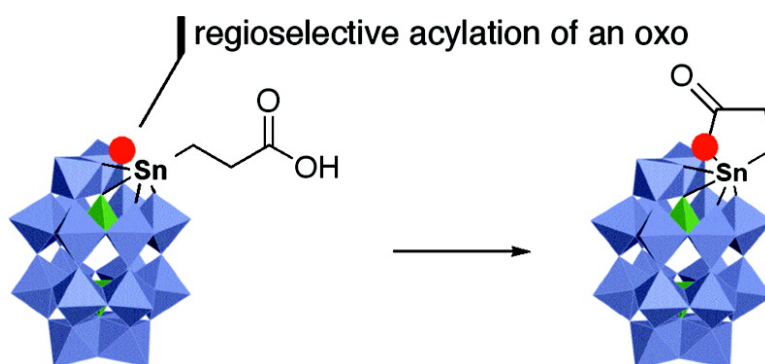


Regioselective Activation of Oxo Ligands in Functionalized Dawson Polyoxotungstates

Ccile Boglio, Kvin Micoine, tienne Derat, Ren Thouvenot, Bernold Hasenknopf, Serge Thorimbert, Emmanuel Lacte, and Max Malacria

J. Am. Chem. Soc., **2008**, 130 (13), 4553-4561 • DOI: 10.1021/ja800072q

Downloaded from <http://pubs.acs.org> on February 8, 2009



More About This Article

Additional resources and features associated with this article are available within the HTML version:

- Supporting Information
- Links to the 4 articles that cite this article, as of the time of this article download
- Access to high resolution figures
- Links to articles and content related to this article
- Copyright permission to reproduce figures and/or text from this article

[View the Full Text HTML](#)



ACS Publications
 High quality. High impact.

Regioselective Activation of Oxo Ligands in Functionalized Dawson Polyoxotungstates

Cécile Boglio,^{†,‡} Kévin Micoine,[†] Étienne Derat,[†] René Thouvenot,[‡]
Bernold Hasenknopf,^{*,‡} Serge Thorimbert,^{*,†} Emmanuel Lacôte,^{*,†} and
Max Malacria[†]

UPMC Univ Paris 06, Laboratoire de chimie organique (UMR CNRS 7611), Institut de chimie moléculaire (FR 2769), C. 229, 4 place Jussieu, 75005 Paris, France and UPMC Univ Paris 06, Laboratoire de chimie inorganique et matériaux moléculaires (UMR CNRS 7071), Institut de chimie moléculaire (FR 2769), C. 42, 4 place Jussieu, 75005 Paris, France

Received January 4, 2008; E-mail: serge.thorimbert@upmc.fr; bernold.hasenknopf@upmc.fr; emmanuel.lacote@upmc.fr

Abstract: The organic side chain of tin-substituted Dawson polyoxotungstates α_1 - and α_2 -[P₂W₁₇O₆₁{SnCH₂-CH₂COOH}]⁷⁻ can be used to direct regioselective acylations of oxo ligands in the inorganic backbone, which was examined both experimentally and computationally. Acylation of the oxo ligand gave exalted electrophilicity to the acyl moiety, and the compounds that were obtained led to direct ligation of POMs to complex organic molecules.

Introduction

Functionalization of the basic structures of polyoxometalates (POMs) by grafting organic molecules is a unique way to install designed additional features that modulate POM properties, which is a key to numerous applications in catalysis, materials science, and potentially chemical biology. Activation of the numerous oxo ligands is an appealing strategy for such a purpose.^{1,2} However, saturated polyoxotungstates remain mostly unreactive toward electrophiles because their charge density is too diffuse for the oxo ligands to be nucleophilic enough.^{3,4} An additional problem is selectivity. By nature, POMs have numerous oxo ligands, and distinguishing them is generally a difficult task. Thus, one generally relies on reactions of lacunary compounds with a more limited number of nucleophilic oxo ligands.

Introduction of designed substituents in the polyoxometallic framework for the orientation of subsequent functionalization is an attractive way to cope with this lack of selectivity. In particular, it has been shown that a metal ion in an oxidation state lower than six increased the nucleophilicity of the attached bridging oxo ligands. Not only was Lindqvist niobotungstate [Nb₂W₄O₁₉]⁴⁻ methylated in a few minutes—its parent [W₆O₁₉]²⁻ did not react under the same conditions—but also the reaction was selective for the oxo ligands that were bound to the Nb(V).³ Klemperer thoroughly used this feature to prepare numer-

ous compounds.^{5–10} However, a mixture of isomers was often generated. A similar effect was observed with a reduced molybdenum species,¹¹ in Nb- and V-containing Keggin or Dawson complexes,^{12–14} and for the acylation of Zn- and Cu-substituted Keggin polyoxotungstates.¹⁵ In this latter case, So obtained mixtures of products from acylations of several W–O–Zn ligands, while all W–O–Cu ligands were acylated. Control of the regioselectivity between oxo ligands with very close reactivities is thus an important milestone to be set for the designed functionalization of tungstates.

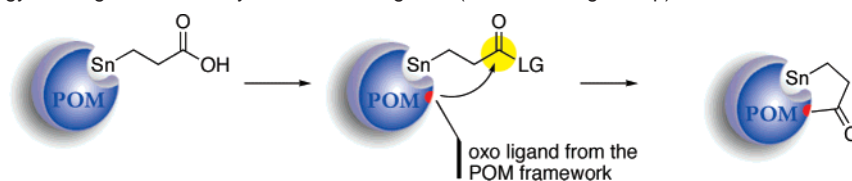
As part of our program focusing on the preparation of polyoxometalates incorporating designed functions,^{16–21} we introduced an ω -carboxyl moiety on the side chain of α_1 - and

- (5) Besecker, C. J.; Day, V. W.; Klemperer, W. G.; Thompson, M. R. *J. Am. Chem. Soc.* **1984**, *106*, 4125–4136.
- (6) Besecker, C. J.; Day, V. W.; Klemperer, W. G.; Thompson, M. R. *Inorg. Chem.* **1985**, *24*, 44–50.
- (7) Besecker, C. J.; Klemperer, W. G. *J. Am. Chem. Soc.* **1980**, *102*, 7598–7600.
- (8) Day, V. W.; Eberspacher, T. A.; Klemperer, W. G.; Planalp, R. P.; Schiller, P. W.; Yagasaki, A.; Zhong, B. *Inorg. Chem.* **1993**, *32*, 1629–1637.
- (9) Day, V. W.; Klemperer, W. G.; Main, D. J. *Inorg. Chem.* **1990**, *29*, 2345–2355.
- (10) Klemperer, W. G.; Main, D. J. *Inorg. Chem.* **1990**, *29*, 2355–2360.
- (11) Proust, A.; Thouvenot, R.; Robert, F.; Gouzerh, P. *Inorg. Chem.* **1993**, *32*, 5299–5304.
- (12) Pohl, M.; Lin, Y.; Weakley, T. J. R.; Nomiya, K.; Kaneko, M.; Weiner, H.; Finke, R. G. *Inorg. Chem.* **1995**, *34*, 767–777.
- (13) Rapko, B. M.; Pohl, M.; Finke, R. G. *Inorg. Chem.* **1994**, *33*, 3625–3634.
- (14) Lee, C. W.; So, H.; Lee, K. R. *Bull. Korean Chem. Soc.* **1988**, *9*, 362–364.
- (15) Hahn, J. S.; So, H. *Bull. Korean Chem. Soc.* **1992**, *13*, 92–94.
- (16) Bareyt, S.; Piligkos, S.; Hasenknopf, B.; Gouzerh, P.; Lacôte, E.; Thorimbert, S.; Malacria, M. *J. Am. Chem. Soc.* **2005**, *127*, 6788–6794.
- (17) Bareyt, S.; Piligkos, S.; Hasenknopf, B.; Gouzerh, P.; Lacôte, E.; Thorimbert, S.; Malacria, M. *Angew. Chem., Int. Ed.* **2003**, *42*, 3404–3406.
- (18) Micoine, K.; Hasenknopf, B.; Thorimbert, S.; Lacôte, E.; Malacria, M. *Org. Lett.* **2007**, *9*, 3981–3984.
- (19) Boglio, C.; Lemièrre, G.; Hasenknopf, B.; Thorimbert, S.; Lacôte, E.; Malacria, M. *Angew. Chem., Int. Ed.* **2006**, *45*, 3324–3327.
- (20) Boglio, C.; Lenoble, G.; Duhayon, C.; Hasenknopf, B.; Thouvenot, R.; Zhang, C.; Howell, R. C.; Burton-Pye, B. P.; Francesconi, L. C.; Lacôte, E.; Thorimbert, S.; Malacria, M.; Afonso, C.; Tabet, J.-C. *Inorg. Chem.* **2006**, *45*, 1389–1398.

[†] Laboratoire de chimie organique.

[‡] Laboratoire de chimie inorganique et matériaux moléculaires.

- (1) (a) Gouzerh, P.; Proust, A. *Chem. Rev.* **1998**, *98*, 77–111. (b) Proust, A.; Thouvenot, R.; Gouzerh, P. *Chem. Commun.* **2008**, DOI: 10.1039/b715502f.
- (2) Long, D.-L.; Burkholder, E.; Cronin, L. *Chem. Soc. Rev.* **2007**, *36*, 105–121.
- (3) Day, V. W.; Klemperer, W. G.; Schwartz, C. *J. Am. Chem. Soc.* **1987**, *109*, 6030–6044.
- (4) Knoth, W. H.; Harlow, R. L. *J. Am. Chem. Soc.* **1981**, *103*, 4265–4266.

Scheme 1 General Strategy for Regioselective Acylation of Oxo Ligands (LG = Leaving Group)

α_2 -tin-substituted Dawson^{16,17} and α -tin-substituted Keggin¹⁸ polyoxotungstates for coupling to designed functional amines.²² It appeared to us that under certain reaction conditions the activated carboxyl group of our scaffolds could be trapped *intramolecularly* by an oxo ligand and thus ensure exclusive *monoacylation* of the POM (Scheme 1).

Oxocarbon derivatives of POMs are known, but they are very rare for tungstates.²³ Carbonates, carboxylates, oxalates, and related ligands are generally structural building units of the polyoxometallic frameworks, where they adopt a bridging binding mode.^{24–27} Aldehydes are converted to their hydrates for binding.^{28,29} To the best of our knowledge, So's are the only examples of acyl-POM derivatives—a carboxylate bound to the metal by only one oxygen.^{14,15}

The stereoelectronic constraints induced in this proposed intramolecular acylation and the probably increased nucleophilicity due to the presence of the Sn(IV) atom should direct the cyclization to specific oxo ligands only. Regioselectivity was hoped for. This increased control over reactions introduced by tethering the reactive partners in stepwise synthesis is common in organic chemistry.³⁰ To the best of our knowledge, there is no report of its extension to POMs nor has the effect of tin functionalization on the control of further functionalization been investigated. We therefore decided to explore the intramolecular acylation of polyoxotungstates by investigating the reactivity of a family of similar organotin–phosphotungstates.

We report herein the regioselective mono-oxoacylation of polyoxotungstates α_1 - and α_2 -[P₂W₁₇O₆₁{SnCH₂CH₂COOH}]⁷⁻, which were regioselectively converted into inorganic lactones to afford doubly functionalized structures (two separate functions introduced sequentially). The Keggin compound α -[PW₁₁O₃₉{SnCH₂CH₂COOH}]⁴⁻ was also investigated. Computational studies have been used to understand the reactivities of the different oxo ligands.

Materials and Methods

Reagents and chemicals were purchased from commercial sources and used as received. Functionalized polyoxometalates TBA₆H[α_1 -P₂W₁₇O₆₁{SnCH₂CH₂CO₂H}] (1) and TBA₆K[α_2 -P₂W₁₇O₆₁{SnCH₂CH₂CO₂H}] (3) were prepared following methods reported in the literature.^{16,18} Unless otherwise noted, reactions were carried out under air atmosphere with magnetic stirring. CH₃CN was dried and distilled from CaH₂. Thin-layer chromatography (TLC) was performed on Merck 60F₂₅₄ silica gel.

Analytical Details. IR spectra were recorded from a Bruker Tensor 27 ATR diamond PIKE spectrophotometer. ¹H NMR [¹³C NMR] spectra were recorded at room temperature with a 400 MHz [100 MHz] Bruker AVANCE 400 spectrometer or a 200 MHz [50 MHz] Bruker AVANCE 200. Chemical shifts are given in ppm, referenced to TMS ($\delta = 0$ ppm) using the solvent signals $\delta = 1.94$ ppm for CHD₃CN [$\delta = 118.3$ ppm for CD₃CN]. Coupling constants (*J*) are given in Hertz (Hz). ³¹P NMR spectra were obtained at 298 K in a 5 mm o.d. tube at 162 MHz on a Bruker AVANCE 400 spectrometer equipped with a QNP or BBFO probe at a concentration of 100 mg/0.5 mL. External 85% H₃PO₄ in a coaxial tube was used as the reference. ¹⁸³W NMR spectra (300 K) were recorded in 10 mm o.d. tubes (sample volume 2.5 mL) at 12.5 MHz on a Bruker Avance II 300 equipped with a low-frequency special VSP probehead and at 20.8 MHz on a Bruker DRX500 spectrometer with a standard tunable BBO probehead. Chemical shifts are referenced to WO₄²⁻ ($\delta = 0$ ppm). They were measured by the substitution method using a saturated aqueous solution (in D₂O) of dodecatungstosilicic acid (H₄SiW₁₂O₄₀) as a secondary standard ($\delta = -103.8$ ppm). ¹¹⁹Sn NMR spectra (300 K) were recorded in 10 mm o.d. tubes at 111.9 MHz on a Bruker Avance II 300 equipped with a standard tunable BBO probehead. Chemical shifts are referenced to (CH₃)₄Sn and were measured by the substitution method. Mass spectrometry experiments have been carried out on an electrospray-ion trap instrument (Bruker, Esquire 3000). The 50 μ mol·L⁻¹ solutions of POMs were infused using a syringe pump (160 μ L·h⁻¹). The negative-ion mode was used with capillary high voltage 3500 V. The orifice/skimmer voltage difference was set to 45 V to avoid decomposition of the POMs. The low mass cutoff (LMCO) of the ion trap was set to 80 Th. (K). Elemental analyses were carried out by the “Service Central d’Analyse”, CNRS, Vernaison, France, or by the ICSN, CNRS, Gif, France.

Computational Details. The TURBOMOLE³¹ software was used to perform the QM (DFT) calculations using the B-P86 functional within the framework of the RI approximation. The SV(P) basis set developed by Ahlrichs³² was used for geometry optimization, and energetic single points were subsequently done with TZVP.³³ Due to the size of the Dawson cluster, frequency calculations were not performed. Only the calculations carried out for the Keggin POMs were checked by frequency analysis. Except for the transition states, no imaginary frequencies were found. Solvent effects induced by acetonitrile and water were taken into account by turning on the COSMO implementation. The dielectric constant was set to 36.64 for acetonitrile and 78.5 for water.

TBA₆[α_1 -P₂W₁₇O₆₁{SnCH₂CH₂C(=O)}] (2). To a solution of TBA₆H[α_1 -P₂W₁₇O₆₁{SnCH₂CH₂CO₂H}] (1, 1.55 mmol, 9.0 g) in CH₃CN (100

- (21) Boglio, C.; Micoine, K.; Rémy, P.; Hasenknopf, B.; Thorimbert, S.; Lacôte, E.; Malacria, M.; Afonso, C.; Tabet, J.-C. *Chem. Eur. J.* **2007**, *13*, 5426–5432.
- (22) Organotin-substituted Dawson polyoxometalates were introduced by Pope: (a) Zonnevijlle, F.; Pope, M. T. *J. Am. Chem. Soc.* **1979**, *101*, 2731–2732. (b) Chorghade, G. S.; Pope, M. T. *J. Am. Chem. Soc.* **1987**, *109*, 5134–5138. (c) Sazani, G.; Pope, M. T. *Dalton Trans.* **2004**, 1989–1994. For recent new advances with tin-containing POMs, see: (d) Bar-Nahum, I.; Etedgui, J.; Konstantinovski, L.; Kogan, V.; Neumann, R. *Inorg. Chem.* **2007**, *46*, 5798–5804. (e) Reinoso, S.; Dickman, M. H.; Kortz, U. *Inorg. Chem.* **2006**, *45*, 10422–10424. The biological activity of organotin-substituted POMs has been examined: (f) Liu, J. F. *Transition Met. Chem.* **1998**, *23*, 93–95. (g) Haiduc, I. *Synth. React. Inorg. Met.* **1999**, *29*, 951–965.
- (23) Errington, R. J.; Kerlogue, M. D.; Richards, D. G. *Chem. Commun.* **1993**, 649–651.
- (24) Chen, Q.; Liu, S.; Zubietta, J. *Angew. Chem., Int. Ed.* **1988**, *100*, 1792–1793.
- (25) Chen, Q.; Liu, S.; Zubietta, J. *Inorg. Chem.* **1989**, *28*, 4433–4434.
- (26) Kortz, U.; Savelieff, M. G.; Ghali, F. Y. A.; Khalil, L. M.; Maalouf, S. A.; Sinno, D. I. *Angew. Chem., Int. Ed.* **2002**, *41*, 4070–4073.
- (27) Mak, T. C. W.; Li, P.; Zheng, C.; Huang, K. *J. Chem. Soc., Chem. Commun.* **1986**, 1597–1598.
- (28) Day, V. W.; Fredrich, M. F.; Klemperer, W. G.; Liu, R. S. *J. Am. Chem. Soc.* **1979**, *101*, 491–492.
- (29) Day, V. W.; Thompson, M. R.; Day, C. S.; Klemperer, W. G.; Liu, R. S. *J. Am. Chem. Soc.* **1980**, *102*, 5971–5973.
- (30) Fensterbank, L.; Malacria, M.; Sieburth, S. M. *Synthesis* **1997**, 813–854.

- (31) Ahlrichs, R.; Bär, M.; Häser, M.; Horn, H.; Kölmel, C. *Chem. Phys. Lett.* **1989**, *162*, 165–169.
- (32) Schäfer, A.; Horn, H.; Ahlrichs, R. *J. Chem. Phys.* **1992**, *97*, 2571–2577.
- (33) Schäfer, A.; Huber, C.; Ahlrichs, R. *J. Chem. Phys.* **1994**, *100*, 5829–5835.

mL) was added NEt_3 (3.4 mmol, 2.2 equiv, 0.48 mL) and isobutylchloroformate (1.86 mmol, 1.2 equiv, 0.24 mL). The mixture was stirred at rt for 3 h. If the reaction was not totally completed as attested by ^{31}P NMR, some more NEt_3 and isobutyl chloroformate were added depending on the conversion and the mixture was stirred one more hour. A cation-exchange resin (Amberlyst 15, 16–50 mesh, TBA^+ form) was added, followed by acetone (10 mL), and the mixture was stirred for 1 h. The resin was filtered off, and the filtrate was concentrated in vacuo. The oil that was obtained was dissolved in acetone (7 mL) and precipitated upon addition of $\text{EtOH/Et}_2\text{O}$ (7 mL/300 mL). The solid was isolated by filtration, washed with Et_2O , and dried in vacuo to afford the desired POM **2** (1.22 mmol, 7.1 g, 79%) as a white powder. IR: $\tilde{\nu}$ = 2962 (m), 2935 (w), 2874 (m), 1721 (w), 1485 (m), 1381 (w), 1152 (w), 1090 (s), 1011 (w), 957 (s), 911 (s), 788 (vs) cm^{-1} . ^1H NMR (400 MHz, CD_3CN): δ 1.08 (t, J = 7.2 Hz, 72 H, $\text{N}[(\text{CH}_2)_3\text{Me}]_4$), 1.38–1.48 (m, 50H, $\text{N}(\text{CH}_2\text{CH}_2\text{CH}_2\text{Me})_4$ + SnCH_2), 1.61–1.68 (m, 48 H, $\text{N}(\text{CH}_2\text{CH}_2\text{CH}_2\text{Me})_4$), 2.84 (m, 2 H, $\text{CH}_2\text{C}=\text{O}$), 3.14–3.20 (m, 48 H, $\text{N}(\text{CH}_2\text{Pr})_4$). ^{13}C NMR (100 MHz, CD_3CN): δ 13.9 ($\text{N}[(\text{CH}_2)_3\text{Me}]_4$), 20.1 (SnCH_2), 20.3 ($\text{N}(\text{CH}_2\text{CH}_2\text{CH}_2\text{Me})_4$), 24.3 ($\text{N}(\text{CH}_2\text{CH}_2\text{CH}_2\text{Me})_4$), 32.4 ($\text{CH}_2\text{C}=\text{O}$), 59.1 ($\text{N}(\text{CH}_2\text{Pr})_4$), 170.2 ($\text{C}=\text{O}$). ^{31}P NMR (162 MHz, CD_3CN): δ -11.9 (s, 1 P), -5.4 (s + d, 1 P, J_{SnP} = 26 Hz). ^{119}Sn NMR (CD_3CN): δ -506.9 (dd, J_{SnP} = 26 Hz, J_{SnW} = 85 Hz). ^{183}W NMR (CD_3CN): δ -98.2, -100.5, -105.9, -108.4, -144.8, -148.7, -158.5, -163.0, -169.5, -172.8 (2 W), -180.4, -191.2, -196.9, -220.1, -244.3, -257.2. Anal. Calcd for $\text{C}_{99}\text{H}_{220}\text{N}_6\text{O}_{62}\text{P}_2\text{SnW}_{17}$ (5792.94 $\text{g}\cdot\text{mol}^{-1}$): C, 20.53; H, 3.83; N, 1.45. Found: C, 20.71; H, 3.85; N, 1.43. ESI⁻/MS: see Supporting Information for full details.

TBA₆[α_2 -P₂W₁₇O₆₁{SnCH₂CH₂C(=O)}] (**4**). To a solution of **TBA₆K[α_2 -P₂W₁₇O₆₁{SnCH₂CH₂CO₂H}]** (**3**, 0.075 mmol, 450 mg) in MeCN (3 mL) was added NEt_3 (0.165 mmol, 2.2 equiv, 0.016 mL) and isobutyl chloroformate (0.113 mmol, 1.5 equiv, 0.015 mL). The mixture was stirred at rt for 3 h. If the reaction was not totally completed as attested by ^{31}P NMR, some more NEt_3 and isobutyl chloroformate were added (quantity depending on the conversion) and the mixture was stirred 1 more hour. A cation-exchange resin (Amberlyst 15, 16–50 mesh, TBA^+ form) was added, followed by acetone (10 mL), and the mixture was stirred for 1 h. The resin was filtered off, and the filtrate was concentrated in vacuo. The remaining oil was dissolved in acetone (3 mL) and precipitated upon addition of $\text{EtOH/Et}_2\text{O}$ (3 mL/50 mL). The solid was isolated by filtration, washed with Et_2O , and dried in vacuo to afford the desired POM **4** (0.068 mmol, 402 mg, 91%) as a white powder. IR: $\tilde{\nu}$ = 2959 (m), 2933 (w), 2872 (m), 1711 (w), 1483 (m), 1379 (w), 1222 (w), 1093 (s), 952 (s), 889 (s), 763 (vs) cm^{-1} . ^1H NMR (400 MHz, CD_3CN): δ 1.08 (t, J = 7.2 Hz, 72 H, $\text{N}[(\text{CH}_2)_3\text{Me}]_4$), 1.26 (m, 2 H, SnCH_2), 1.38–1.48 (m, 48H, $\text{N}(\text{CH}_2\text{CH}_2\text{CH}_2\text{Me})_4$), 1.61–1.68 (m, 48 H, $\text{N}(\text{CH}_2\text{CH}_2\text{CH}_2\text{Me})_4$), 2.72 (m, 2 H, $\text{CH}_2\text{C}=\text{O}$), 3.14–3.20 (m, 48 H, $\text{N}(\text{CH}_2\text{Pr})_4$). ^{13}C NMR (100 MHz, CD_3CN): δ 13.9 ($\text{N}[(\text{CH}_2)_3\text{Me}]_4$), 18.0 (SnCH_2), 20.3 ($\text{N}(\text{CH}_2\text{CH}_2\text{CH}_2\text{Me})_4$), 24.3 ($\text{N}(\text{CH}_2\text{CH}_2\text{CH}_2\text{Me})_4$), 31.9 ($\text{CH}_2\text{C}=\text{O}$), 59.1 ($\text{N}(\text{CH}_2\text{Pr})_4$), 170.4 ($\text{C}=\text{O}$). ^{31}P NMR (162 MHz, CD_3CN): δ -12.2 (s, 1 P), -10.0 (s + d, 1 P, J_{SnP} = 24 Hz). ^{119}Sn NMR (CD_3CN): δ -465.9 (dd, J_{SnP} = 25 Hz, J_{SnW} = 52 Hz). ^{183}W NMR (CD_3CN): δ -70.5, -99.2, -114.6, -143.1, -147.6, -152.2, -157.9, -160.1, -169.2, -171.0, -172.2, -176.9, -187.3, -190.7 (2W), -197.2, -230.2. Anal. Calcd for $\text{C}_{99}\text{H}_{220}\text{N}_6\text{O}_{62}\text{P}_2\text{SnW}_{17}$ (5792.94 $\text{g}\cdot\text{mol}^{-1}$): C, 20.53; H, 3.83; N, 1.45. Found: C, 20.50; H, 3.60; N, 1.51. ESI⁻/MS: see Supporting Information for full details.

Results and Discussion

We modified our initial [α_1 -P₂W₁₇O₆₁{SnCH₂CH₂COOH}]⁷⁻ (**1**) carboxyl activation protocol¹⁶ by replacing *t*BuOK with triethylamine as the base to scavenge the proton released. A new POM **2** was isolated in 79% yield from **1**. Its ^{31}P NMR spectrum showed two signals in the expected region for substituted Dawson POMs, and $J_{\text{P-Sn}}$ coupling proved that the

polyoxotungstic framework was not affected. Further confirmation of this POM structure came from the IR spectrum and the 17-line ^{183}W NMR spectrum. Chemical shifts for **2** were different from **1** but in the normal range for diamagnetic phosphotungstates (Figure 1). ^{119}Sn NMR showed a signal at -506.9 ppm for **2** compared to -551.5 ppm for **1**. Its ^1H NMR and ^{13}C NMR spectra were similar to that of the starting compound, i.e., showing only two methylene and one carbonyl groups, a good hint that the cyclization had taken place (see Supporting Information). Negative-mode ESI-MS suggested the loss of a hydroxyl moiety in **2**.

Most importantly, the well-resolved NMR spectra of all the nuclei observed indicated a single compound. Thus, cyclization of a backbone oxygen to the activated carboxylic acid yielded a doubly functionalized POM (**2**) with total regioselectivity. Even if there were reasons to expect closure onto only a few oxo ligands (out of the 53 external ligands in the Dawson structure) owing to the higher nucleophilicity of W–O–Sn bridging ligands and the length of the tether, this outcome was still surprising since it was not obvious that the four different W–O–Sn bridges should behave so differently. In addition, the *intramolecular* approach made the reaction stop at monoacylation of the POMs.

We decided to examine this in more detail as it should give deeper insight into the reactivity of Dawson polyoxotungstates. Where relevant, we decided to approach these issues also from a theoretical point of view by QM (DFT) calculations. This was very challenging because of the very high number of heavy atoms involved, and it was not clear whether efficient and reliable methodologies could provide a good description of the reactivity of molecular species as large as Dawson POMs.

The following issues needed to be addressed: (i) What is the scope of the regioselective monoacylation? (ii) Which oxo ligand is involved in the cyclization? (iii) What is the mechanism of the reaction? (iv) Is the tether really needed? (v) What is the reactivity of the cyclized products?

1. Scope of the Intramolecular Acylation. In addition to the α_1 -Dawson derivative **1**, we examined two related POMs: the isomeric achiral α_2 -[P₂W₁₇O₆₁{SnCH₂CH₂COOH}]⁷⁻ (**3**) and the Keggin derivative α -[PW₁₁O₃₉{SnCH₂CH₂COOH}]⁴⁻ (**5**). Our purpose was to examine the relative roles of the charge and geometries of the polyanions.

Under similar activation conditions as for the preparation of **2** (NEt_3 , 2.2 equiv; chloroformate, 1.5 equiv; room temperature; 4 h), **3** yielded 90% of acylated POM **4** as a unique product. Again, ^{31}P NMR and IR indicated the intact α_2 -Dawson framework, and the signal of ^{119}Sn NMR was deshielded (-465.9 ppm for **4** compared to -494.7 ppm for **3**, Figure 2). Interestingly, the α -carbonyl ^1H NMR signal went from a triplet in **3** (coupling with two equivalent SnCH₂ protons) to a much more complicated ABXY system in **4** (two diastereotopic protons, Figure 3). This demonstrates that **4** is chiral, and this was further confirmed by the 17-line ^{183}W NMR spectrum (Figure 2). This is unambiguous proof that the mirror plane of the α_2 -Dawson isomer is suppressed by the reaction of the POM framework. Consequently, the transformation of **3** to **4** corresponds to a regioselective intramolecular cyclization leading to a chiral compound. ESI-MS is in agreement with this formulation.

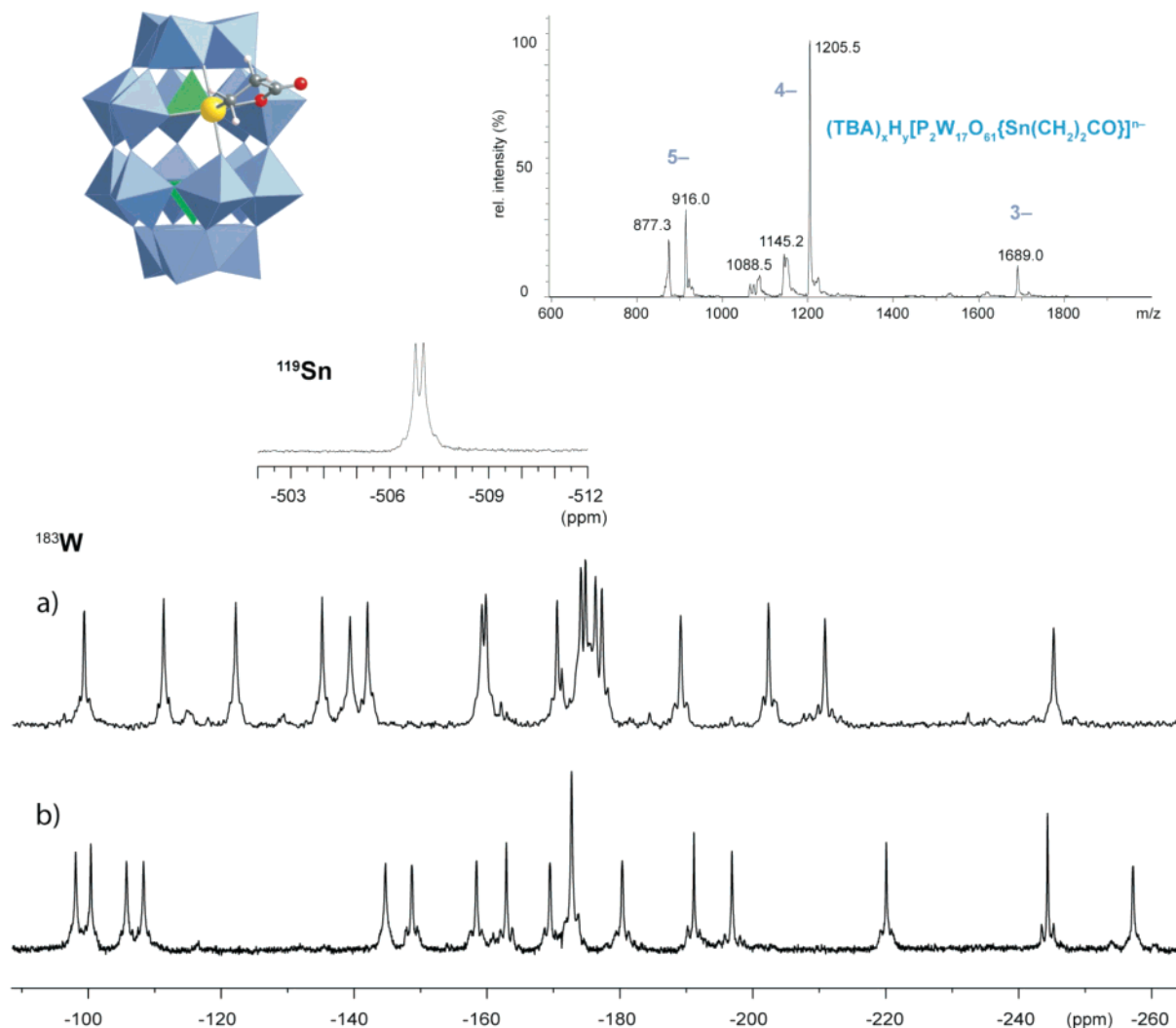


Figure 1. Spectroscopic characterization of **2** (structure drawn from the calculations, see below); ESI-MS; ^{119}Sn NMR (CD_3CN , 1.4 g/mL; ^{183}W NMR: (a) POM **1** for comparison (CD_3CN , 1.3 g/mL) and (b) **2** (CD_3CN , 1.4 g/mL). See Experimental Section for details.

Surprisingly, no cyclization was observed for the Keggin anion $[\text{PW}_{11}\text{O}_{39}\{\text{SnCH}_2\text{CH}_2\text{CO}_2\text{H}\}]^{4-}$, **5**. The only isolated POM (**6**) after cation exchange with a TBA-loaded amberlyst resin was the mixed anhydride (Figure 4).

The lactonization could be performed without activating agent. POM **3** yielded 55% of **4** by simple heating in a microwave oven. Unfortunately, some degradation took place and **4** could not be isolated pure by this route. POM **1** did not cyclize into **2** under these conditions. Seventy-five percent of **1** was recovered. α_1 to α_2 isomerization of **1** into **3** was not observed. Even if those conditions are yet to be refined to lead to synthetically useful and preparative transformations, microwave irradiation is a promising avenue for POM functionalization.³⁴

2. Regioselectivity of the Intramolecular Acylation. Determination of the activated oxo ligand was a more challenging issue. The acylated POMs **2** and **4** could not be crystallized, and the spectroscopic results gave only limited information. In both cases, the large shift of the ^{119}Sn nucleus, the variation of the $^2J_{\text{Sn}-\text{W}}$ coupling constants, the length of the tether, as well as the published results from the literature^{4,15} argue for

acylation occurring on a W–O–Sn bridge. To obtain further insight and discriminate between the four W–O–Sn ligands, we decided to look at the problem from a theoretical point of view.

Previous theoretical studies on POMs have shown DFT calculations to be helpful to analyze their structures^{35–38} or understand their reactivities.^{39–42} One question that arises when doing calculations with negatively charged clusters like Dawson heteropolyanions is the importance of the solvent effect. A previous study by Poblet showed that it is necessary to include at least nonspecific solvent effects (through COSMO or PCM models) when the ratio (charge/number of metal centers) is

(35) Lopez, X.; Maestre, J. M.; Bo, C.; Poblet, J. M. *J. Am. Chem. Soc.* **2001**, *123*, 9571–9576.

(36) Maestre, J. M.; Lopez, X.; Bo, C.; Poblet, J. M.; Casañ-Pastor, N. *J. Am. Chem. Soc.* **2001**, *123*, 3749–3758.

(37) Poblet, J. M.; Lopez, X.; Bo, C. *Chem. Soc. Rev.* **2003**, *32*, 297–308.

(38) Musaev, D. G.; Morokuma, K.; Geletii, Y. V.; Hill, C. L. *Inorg. Chem.* **2004**, *43*, 7702–7708.

(39) de Visser, S. P.; Kumar, D.; Neumann, R.; Shaik, S. *Angew. Chem., Int. Ed.* **2004**, *43*, 5661–5665.

(40) Kumar, D.; Derat, E.; Khenkin, A. M.; Neumann, R.; Shaik, S. *J. Am. Chem. Soc.* **2005**, *127*, 17712–17718.

(41) Derat, E.; Kumar, D.; Neumann, R.; Shaik, S. *Inorg. Chem.* **2006**, *45*, 8655–8663.

(42) Prabhakar, R.; Morokuma, K.; Hill, C. L.; Musaev, D. G. *Inorg. Chem.* **2006**, *45*, 5703–5709.

(34) Bagno, A.; Bonchio, M.; Sartorel, A.; Scorrano, G. *Eur. J. Inorg. Chem.* **2000**, 17–20.

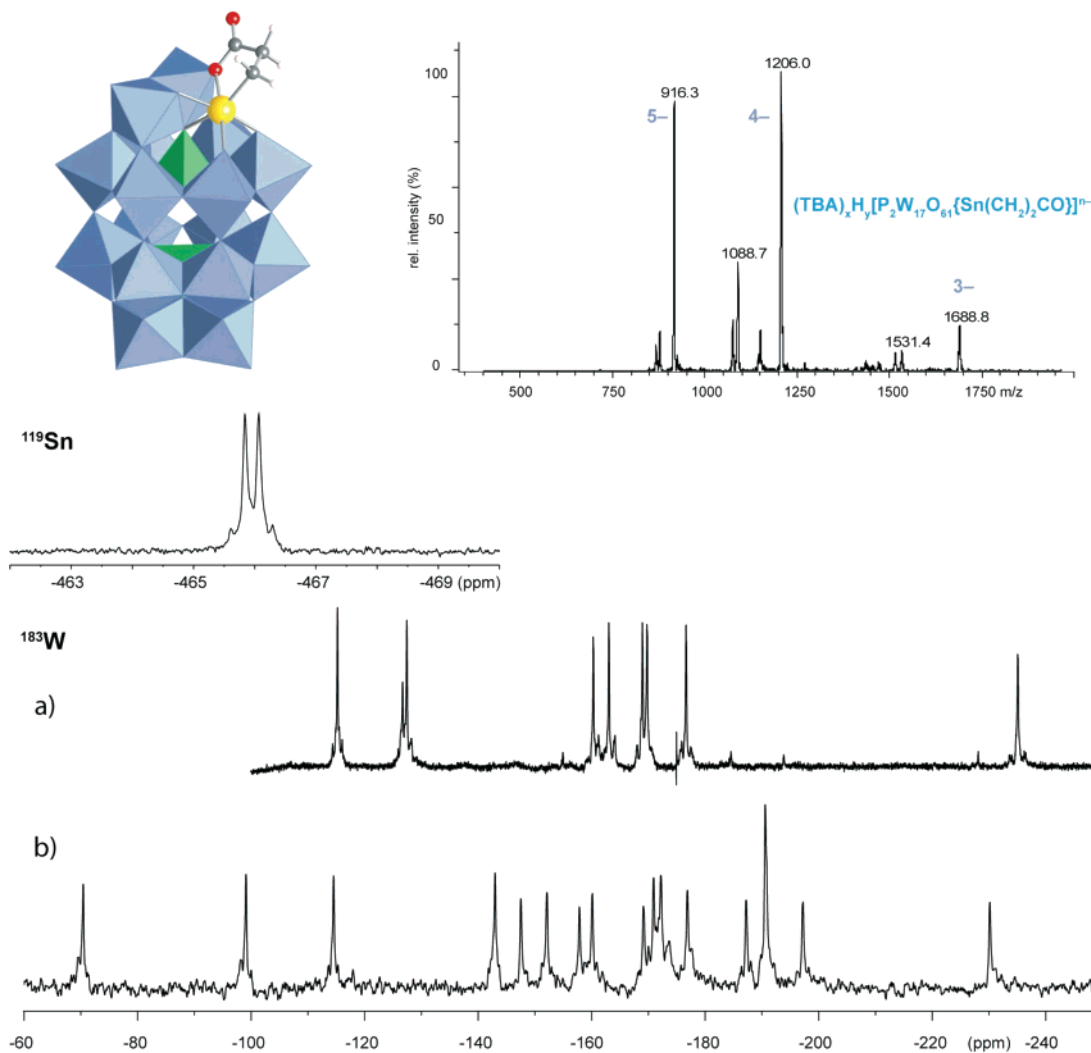


Figure 2. Spectroscopic characterization of **4** (structure drawn from the calculations, see below); ESI-MS; ^{119}Sn NMR (CD_3CN , 0.6 g/mL); ^{183}W NMR: (a) POM **3** for comparison (CD_3CN , 1.0 g/mL) and (b) **4** (CD_3CN , 0.6 g/mL). See Experimental Section for details.

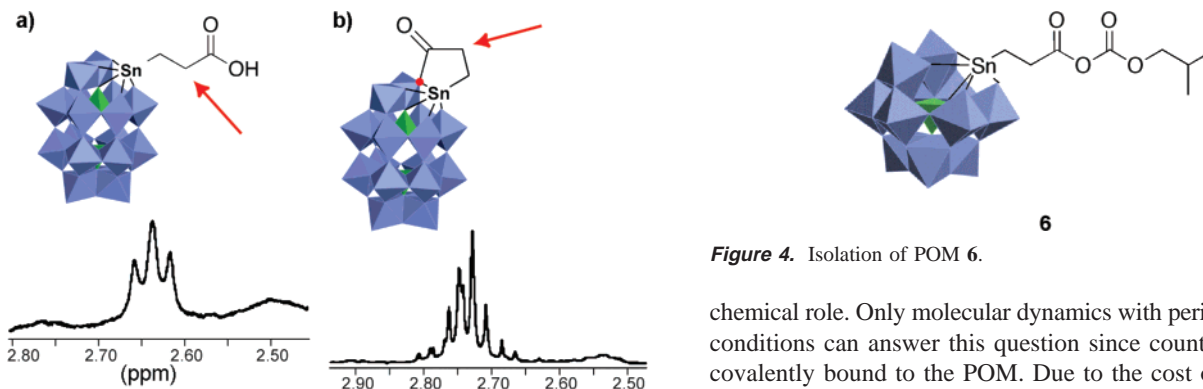


Figure 3. Significant ^1H NMR data for **4**. Comparison of the α -carbonyl protons signals in **3** (a) and **4** (b). All spectra were taken in CD_3CN .

superior to 0.8.⁴³ In the case of Dawson derivatives **2** and **4**, the ratio is $6/18 = 0.33$. Therefore, the solvent effect should be moderate, but we will see that in some cases it is important to explain reactivity. The effect of counterions is also an issue.⁴⁴ Their proximity to the POM may give them an important

(43) Lopez, X.; Fernandez, J. A.; Romo, S.; Paul, J.-F.; Kazansky, L.; Poblet, J. M. *J. Comput. Chem.* **2004**, *25*, 1542–1549.

(44) Rocchiccioli-Deltcheff, C.; Fournier, M.; Franck, R.; Thouvenot, R. *Inorg. Chem.* **1983**, *22*, 207–216.

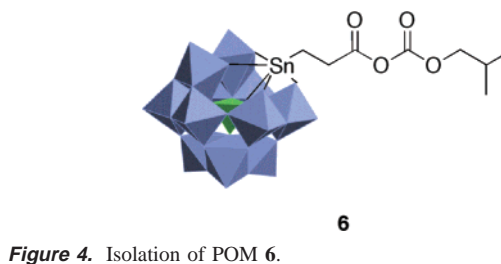


Figure 4. Isolation of POM **6**.

chemical role. Only molecular dynamics with periodic boundary conditions can answer this question since counterions are not covalently bound to the POM. Due to the cost of this type of calculations within the QM framework, it is unfortunately currently still out of reach for POM systems.

Case of 4. The α_2 complex **3** has C_s symmetry. As stated before, the only suitable oxygen atoms available for cyclization are the ones that are bound to the tin atom (Scheme 2). Thus, there are two options: the activated carboxyl can react either with a cap/belt bridging Sn–O–W oxo (**A**) or with a cap/cap bridging Sn–O–W oxo (**B**). We analyzed both possibilities.

In order to compare accurately the relative stabilities of the POM framework in the two regioisomers, the side-chain conformation was maintained identical. As expected, the acyl-

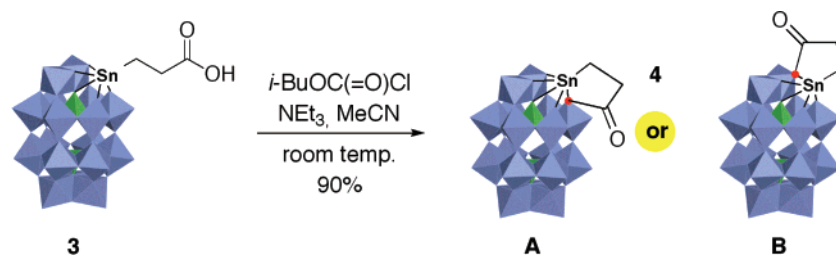
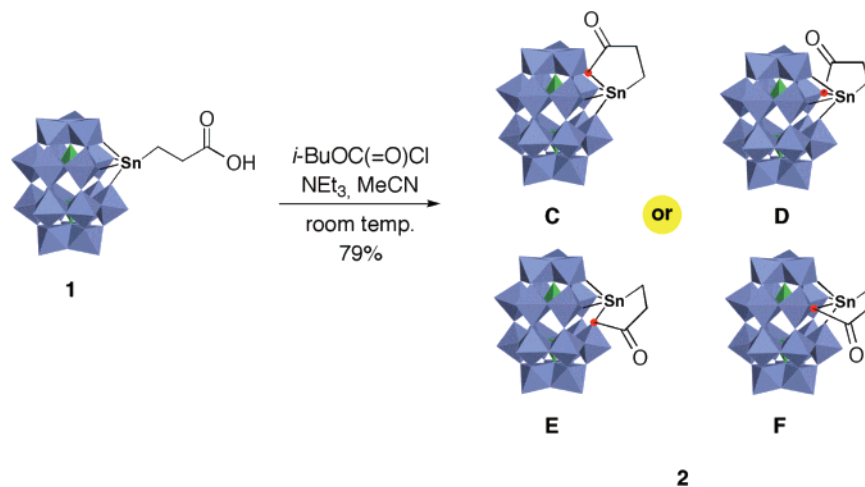
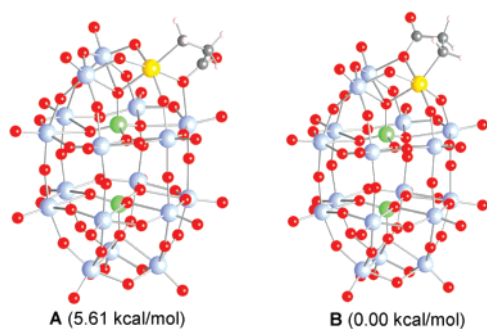
Scheme 2 Cyclization of Sn-Substituted α_2 -Dawson Heteropolyanion **3**Scheme 3 Intramolecular Acylation of Sn-Substituted α_1 -Dawson Heteropolyanion **1**

Table 1. Bond Distances and Angles in Geometry Optimized Structures

POM	W–O (Å)		Sn–O (Å)		W–O–Sn (deg)	
	3	4	3	4	3	4
A	1.89	2.36	2.09	2.31	143.0	126.4
B	1.91	2.26	2.13	2.33	116.9	108.2
POM	1		2		1	
	1	2	1	2	1	2
C	1.88	2.26	2.13	2.43	141.7	124.3
D	1.89	2.19	2.11	2.33	118.2	109.2
E	1.86	2.29	2.09	2.42	159.8	133.2
F	1.87	2.27	2.08	2.37	144.3	123.0

Figure 5. Optimized structures for the two possible regioisomers of heteropolyanion **4** (α_2 -Dawson), calculated at the RI-BP86/SV(P) level.

ation is accompanied by a lengthening of the Sn–O bond from 2.09 (cap-belt oxygens) and 2.13 Å (cap oxygens) in **3** to 2.31 Å in **A** and 2.33 Å in **B** (Table 1). Also, the W–O bond is lengthened by acylation from, respectively, 1.89 and 1.91 Å to 2.36 and 2.26 Å, and the W–O–Sn angle decreases (in **A** from 143.0° to 126.4°; in **B** from 116.9° to 108.2°). This distortion propagates through the whole structure by the *trans* effect. The

W–O bond in the *trans* position to the acylated oxo is shortened, which in turn lengthens the next W–O distance, etc. This calculated distortion of the entire POM is in agreement with the chemical shift variations of all W atoms in ^{183}W NMR spectra, even of those remote of the reactive site. The same phenomenon occurs in mixed-metal Dawson compounds, where local substitutions also influence the chemical shifts of remote nuclei.⁴⁵ The calculated energy is significantly lower (5.61 kcal/mol) when acylation takes place at the cap oxygens, so **B** is the privileged regioisomer of **4**. This is the net result of all bond distortions and cannot be attributed only to a local perturbation of the POM framework.

Case of 2. The starting α_1 complex **1** is chiral; thus, all oxygen atoms are nonequivalent. Again, because the cap/belt bridging W–O–W atom is too far away from the acyl carbon atom (>3 Å) and the electronic effects introduced by the initial functionalization, only the four distinct W–O–Sn bridges had to be considered as reactive sites (Scheme 3).

As before, acylation of an oxo ligand lengthens its Sn–O and W–O bonds and decreases the W–O–Sn angle (Table 1), and this perturbation propagates through the whole framework (Figure 6). The decrease of the bond angle is particularly pronounced for the oxo ligand that bridges the PW_8Sn and PW_9 moieties, which contributes to the instability of isomer **E**. Isomers **C** and **D** are of similar low energy, and the calculations do not allow predicting which of the two is formed in the reaction. One might notice the similar arrangement of **D** and **B** (the most stable isomer in the α_2 case) with the organic ligand within an edge-sharing Sn–W group. This is in accordance with the regioselectivity of oxalkylation in Keggin ions which took

(45) Contant, R.; Abbessi, M.; Thouvenot, R.; Hervé, G. *Inorg. Chem.* **2004**, *43*, 3597–3604.

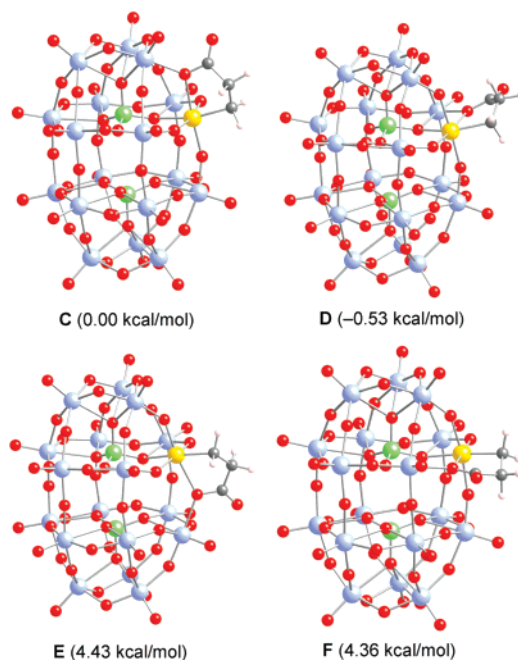


Figure 6. Optimized structures for the four regioisomers of the acylated Sn-substituted heteropolyanion **2** (α_1 -Dawson), calculated at the RI-BP86/SV(P) level.

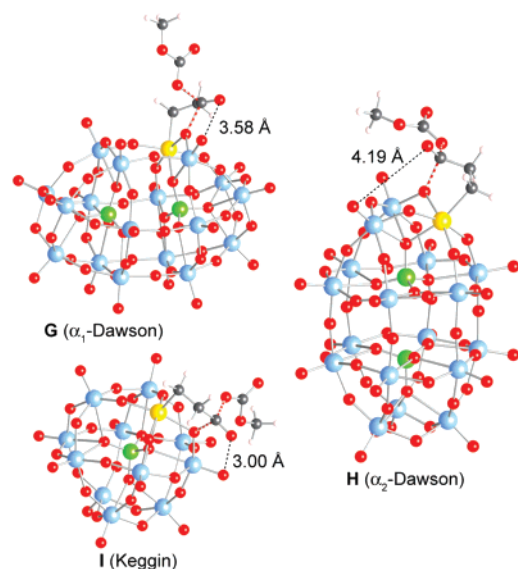


Figure 7. Calculated transition states in the α_1 -Dawson (**G**), α_2 -Dawson (**H**), and Keggin (**I**) cases.

place at bridging oxo ligands between two edge-sharing molybdenum octahedra.⁴

3. Mechanism. We were surprised by the reactivity difference between the Dawson and Keggin ions, and this prompted us to calculate the energies of acetylated Keggin phosphotungstates. The two regioisomers involving the W–O–Sn oxygens either in the SnW_2 trimetallic group or toward a W_3 group were considered. Calculations converged to minima, the lower one involving reaction in the same trimetallic group, a situation reminiscent of **4B** and **2D**. Accordingly, the cyclized product would be stable if it was formed. Thus, the explanation for the reactivity pattern appeared to be related to the activation barrier leading to the cyclization. The precursors for this step are logically the mixed anhydrides, such as **6**, which was isolated

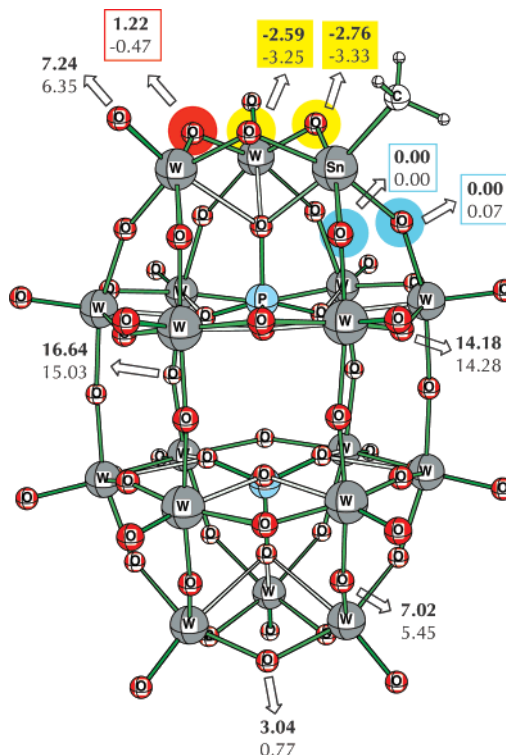


Figure 8. Relative energies of the propanoyl ($\text{CH}_3\text{CH}_2\text{C}(=\text{O})$) derivative (Me)Sn-substituted α_2 -Dawson heteropolyanion **7**, calculated, respectively, at the RI-BP86/SV(P) (bold) and RI-BP86/TZVP//RI-BP86/SV(P) levels. Values are in kcal/mol. All the different oxo atoms were considered.

Table 2. Calculated Activation Energies for the Three Double Activations (Keggin, α_1 -Dawson, α_2 -Dawson) in Gas Phase and with Implicit Solvent Effect. Level: RI-BP86/SV(P) (kcal.mol⁻¹)

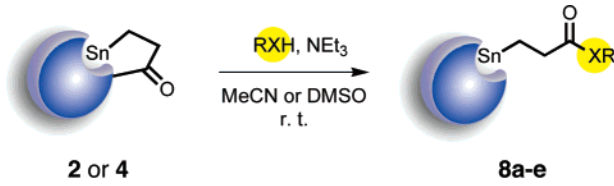
ΔH^\ddagger	gas phase	acetonitrile (COSMO)	water (COSMO)
Keggin	13.98 (13.71 ^a)	19.37	19.52
α_1 -Dawson	14.51	17.65	17.74
α_2 -Dawson	6.26	12.32	12.49

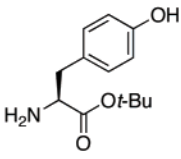
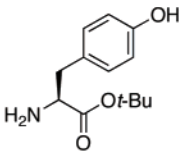
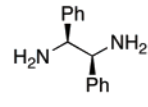
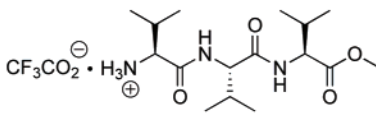
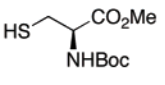
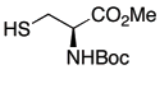
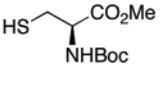
^a The value in parentheses includes the ZPC.

in the Keggin case. Gas-phase transition states to the most stable isomers were sought and located at 14.5 for **2** (see **G**, Figure 7), 6.26 for **4** (see **H**, Figure 7), and 14.0 kcal/mol for the Keggin case (see **I**, Figure 7), which do not reflect the observed reactivities. We thus had to include solvent effects. This led to an increase of all calculated activation energies (Table 2).

Cyclization of the activated derivative of α_2 -Dawson ion **3** was most affected, but its calculated energy remained the lowest in the series. The transition state toward cyclization of the Keggin derivative **5** ended up being the highest of the three POMs. No single-parameter explanation can be found for this behavior. Unfortunately, deeper computational analysis is impossible for those big polyanions.

From our calculations, the POM geometry seems also important as **2** has a considerably higher calculated TS than **4**. On the basis of the previous calculations, the oxygen of the carbonyl approaches the oxo ligands of the framework. While it remains relatively far from any oxo atom in the α_2 -Dawson case (4.19 Å, see **H**), it is much closer in the α_1 -Dawson case (3.58 Å, see **G**) and the Keggin case (3.00 Å, see **I**). This correlates well with the calculated barriers, and it can be related to the observed difference in reactivity of both Dawson

Table 3. Reactivity of the Cyclized POMs **2** and **4**


Entry	POM	RXH	Solvent	Product	Yield (%)
1	4	<chem>H2N-CH2-CH2-CH2-N3</chem>	MeCN	8a (α_2)	88
2	2		MeCN	8b (α_1)	86
3	2		DMSO	8b (α_1)	86
4	2		MeCN	8c (α_1)	94
5 ^a	4		MeCN	8d (α_2)	84
6	2		MeCN	- ^b	-
7 ^c	4		MeCN	8e (α_2)	84
8 ^c	2		MeCN	8f (α_1)	73

^a Cat. DMAP (0.5 equiv) and NEt₃ (4 equiv) were added (see Supporting Information for details). ^b No reaction. ^c Cat. DMAP (0.5 equiv) was added (see Supporting Information for details).

complexes **1** and **3** under microwave irradiation. Only the α_2 isomer **3** cyclized under those conditions (vide supra).

4. Role of the Tether. One clear advantage of using a tethered electrophile is that it ensured clean monoacylation. In order to obtain a more detailed picture of the influence of the spacer, we calculated the energies of an untethered mono-acylated tin-substituted α_2 -Dawson compound. To simplify the calculations, they were carried out on the methylstannyl compound [α_2 -P₂W₁₁O₆₁SnMe], and propanoyl chloride was chosen as the acylating agent. The lack of constraints in **7** prompted us to examine all oxo atoms (Figure 8). We first determined that the

terminal oxo atoms as well as those connecting the PW₈Sn and PW₉ subunits were not conducive to acylation. W–O–W bridging oxygens away from the tin substituent led to low calculated stabilities, which we confirmed experimentally by the absence of reactivity of [P₂W₁₈O₆₂]⁶⁻ under our acylation conditions. This agrees well with the reported higher nucleophilicity of bridging oxo ligands and overall lack of reactivity of tungstates.^{4,14} However, one should note that the acylated W–O–W bridge in the Sn-containing cap of **7** has a calculated stability within the margin of error relative to that of the Sn–O–W cap-belt oxygens. The highest stability is found for the

cap Sn–O–W oxo ligands. Thus, the latter should be the most likely site for acylation in **7**, and it is in good agreement with the results obtained for **4**. Nonetheless, the calculated stability difference between the different W–O–Sn is lower than for the tethered acylation. From this simulation, one could anticipate multiple acylation, as observed by So on Keggin derivatives.¹⁵ Unfortunately, we could not isolate any intermolecularly acylated POM pure enough for unambiguous characterization. TS calculations would provide another insight. Yet, as before, they are hugely time consuming and cannot be carried out for all the systems. Still, the stability pattern is in favor of our initial assumptions that tin substitution should have a good orienting effect, albeit with the caveat that complete regioselectivity is not warranted. *Therefore, the latter is achieved thanks to the tether.*

5. Reactivity of the Cyclized POMs. We decided to look more closely at the reactivity of the cyclized POMs. In particular, trapping of the acyl group by a nucleophile should lead to organic hybrids, in contrast to So's acylated POMs, whose organic functionalization was removed upon amide formation.¹⁵

In a typical experiment (Table 3, entry 1), POM **4** was reacted with a primary amine in the presence of a base. No nucleophilic catalyst was required, and carbophilic attack took place. POM **8a** was obtained in high yield after cation exchange on resin (88%). This exalted electrophilicity may explain why we failed to get crystals from **2** or **4**. Residual water may act as a nucleophile that would reopen the hydrolytically unstable mixed lactone to the ω -carboxyl derivatives.^{14,15}

The reaction tolerates densely functionalized organics (entries 1, 2, 4, and 5). It worked equally well in DMSO (compare entries 2 and 3). The direct reaction from **1** or **3** in DMSO was not possible since DMSO reacts with the activating agents used for carboxylic acids. In all cases, a proton is released that may remain around the polyoxometalate or be trapped by triethylamine or DMAP when present. Thus, all products were converted to their TBA salts by cation-exchange resin.

Overall, as expected, the POM framework acts as an *inorganic* nucleophilic activating agent. This opens interesting

opportunities for further studies, especially for chemical ligation of POMs to amine termini of sensitive biomolecules or molecules not soluble in acetonitrile. Gratifyingly, we could also graft thiols to the POMs, albeit only when DMAP was added (entries 6–8). Thioesters **8e–f** are suitable for ligation to terminal cysteines of proteins, which we are currently examining.

Conclusion

We introduced a new strategy to regioselectively access bis-functionalized Dawson polyoxotungstates through nucleophilic displacement of a tethered electrophile by only one oxo group (out of 53). Computer modeling and spectroscopic analyses were used to evidence which oxo atom reacted and why a similar reactivity was not observed in the corresponding Keggin series. The polyoxometallic framework behaved as an inorganic acyl-activating agent, and highly functionalized hybrid amides and thioesters were obtained through nucleophilic attack of the carbonyl moiety. This selectivity was achieved thanks to the tether, which clearly establishes that the organic appendage does play a primary role in hybrid POM reactivities and that POMs still present fundamentally novel challenges in synthesis. Work to further extend the tethering strategy in POM chemistry, confirm the calculated structures by crystal structures, and use this reagent-free ligation to organic substrates is underway in our laboratories. Progress will be reported in due course.

Acknowledgment. We thank CNRS, IUF, UPMC, le ministère de l'éducation nationale, de l'enseignement supérieur et de la recherche, and ANR (grant JC05_41806 to E.L., S.T., and B.H.) for financial support. Help from Dr. Carlos Afonso and Prof. Jean-Claude Tabet (UPMC) for the mass spectra and Dr. Elsa Caytan (UPMC) for NMR analyses is gratefully acknowledged. E.D. thanks M. Warchol for assistance.

Supporting Information Available: Further synthetic procedures, full characterization of all new compounds, and details of computational analyses. This material is available free of charge via the Internet at <http://pubs.acs.org>.

JA800072Q